Manufacturing Letters 37 (2023) 12–16

Contents lists available at ScienceDirect

Manufacturing Letters

journal homepage: www.elsevier.com/locate/mfglet

Letters

Effect of aging time on mechanical and functional properties of graded Ti-Ni alloy joined by laser additive manufacturing

Yitao Chen [a,*], Cesar Ortiz Rios [b], Frank Liou [a]

[a] Department of Mechanical and Aerospace Engineering, Missouri University of Science and Technology, Rolla, MO 65409, United States
[b] Department of Materials Science and Engineering, Missouri University of Science and Technology, Rolla, MO 65409, United States

ARTICLE INFO

Article history:
Received 2 April 2023
Received in revised form 20 May 2023
Accepted 20 May 2023
Available online 1 June 2023

Keywords:
Functionally Graded Materials
TiNi Alloy
Shape Memory Alloy
Directed Energy Deposition
Metal Joining

ABSTRACT

In this work, a functionally graded Ti-Ni alloy was fabricated using directed energy deposition by depositing Ti-rich Ti-Ni alloy section on near-equiatomic TiNi substrate to demonstrate multi-sectional microstructural, thermal, and mechanical behaviors for multifunctionality. The aging effect at 400 °C with various heat treatment time durations on the graded Ti-Ni alloy was applied. Materials characterization indicated that the two sections demonstrate different responses under various aging treatments, which provided more possible combinations of functional properties in a joined component. This work shows a powerful potential application in using directed energy deposition to fabricate multifunctional smart alloys followed by aging treatment.

1. Introduction

Directed energy deposition (DED) is an important metal additive manufacturing (AM) processes that can fabricate 3D metal parts, join multiple metals, and perform repairing [1,2]. The high material flexibility in DED makes it also capable of developing novel alloys from powder materials. For instance, high entropy alloys and functionally graded alloys that are difficult in conventional processing, have been successfully fabricated by DED [3,4]. Ti-Ni alloy is a popular shape memory alloy (SMA) that is possible to be fabricated by DED [5,6]. Since DED has a high flexibility to build one alloy on another different alloy substrate, it is also possible to build graded Ti-Ni alloy with different behaviors together to realize multi-sectional properties [7]. There is limited work that investigates multi-sectional behaviors under various heat treatment processes. In this work, we attempt to apply the DED process to deposit Ti-Ni alloy on a TiNi substrate with different compositions to develop functionally graded Ti-Ni alloy and investigate the post-aging treatment on the two sections of the graded alloy to reveal the various combination of functional properties. For the DED process, the raw materials were selected as the powder mixture of Ti and Ni powders, which was reported to be an economical way to develop novel alloys from DED [8].

2. Methods

The graded Ti-Ni alloy was fabricated using a laser AM system equipped with an IPG CW fiber laser, an electrostatic powder feeder, and a CNC-controlled gantry. A 25 mm × 9 mm × 5 mm commercial near-equiatomic TiNi piece was used for substrate. Ti and Ni elemental powders with a pre-mixed atomic composition of Ti53Ni47 were homogenized by a Turbula mixer for 30 min. The powder feed rate was 0.9 g/min. The laser was applied to build the Ti-rich Ti-Ni section layer by layer with the back-and-forth single-track multi-layer scan strategy. Laser power was 600 W for the first 7 layers and 500 W for the rest layers. After 100 layers, a Ti-rich Ti-Ni single wall with an average height of 5 mm and 25 mm length was deposited (Fig. 1a). The as-built graded Ti-Ni alloy was sectioned by electrical discharged machining (EDM) for aging treatment. One piece was kept at as-deposited state, and other four pieces experienced 400 °C aging treatment for 0.5hr, 1hr, 2hr, and 5hr in a Marshall tube furnace with argon. All five specimens were then applied for microstructural, thermal, and hardness analysis, especially at the regions near the interface. Specimens for microstructural analysis were prepared following grinding, polishing, and etching with Kroll's reagent ($HF:HNO_3$: H_2O = 2:6:92 vol%) for 30 s. The specimens were imaged by Hirox optical microscope (OM) and TFS Hydra scanning electron microscope (SEM) with energy dispersive spectroscopy (EDS). The phase information was revealed by X-ray diffraction (XRD). Transformation temperatures (TTs) of the interfacial sections, including both

* Corresponding author.
E-mail address: yc4gc@mst.edu (Y. Chen).

https://doi.org/10.1016/j.mfglet.2023.05.003
2213-8463/

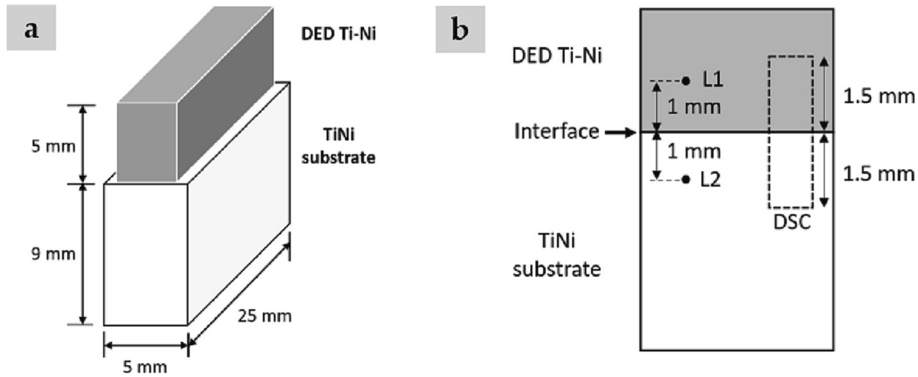

Fig. 1. (a) The schematic of the DED process. (b) The location information of the DSC specimen and hardness.

the DED Ti-Ni half and the substrate half under all aging conditions, were conducted by differential scanning calorimetry (DSC). DSC specimens for all aging states consist of 1.5 mm above and below the interface (Fig. 1b, not drawn in scale). Hardness tests for all aging conditions were carried out at locations 1 mm above (L1) and 1 mm below the interface (L2).

3. Results and discussions

The microstructural and phase information provided by OM, SEM, and XRD is summarized in Fig. 2. Fig. 2a is obtained from the cross-section of the as-deposited DED section, where the layer-wise microstructural distribution and columnar grains can be observed [9]. Fig. 2b focuses on the interface between the two sections including the interfacial line. The area above the interfacial line shows a columnar structure, while the other section consists of equiaxed grains. Fig. 2c is an SEM image of the DED section with matrix and secondary phases. Fig. 2d shows the higher magnification for EDS. Area 2 and Point 3 are selected within the matrix and the secondary phase, while Area 1 represents a larger area including both phases. The Ti/Ni atomic composition of Area 2 and Point 3 are recorded as 51.1%/48.9% and 65.1%/34.9%, respectively. This reflects that Area 2 is Ti-rich TiNi matrix, while Point 3 is Ti_2Ni intermetallic. The atomic composition of Ti and Ni within the larger Area 1 is Ti52.8Ni47.2, which is close to the as-mixed composition. Fig. 2e,f are OM images obtained from the near interface substrate region, where Fig. 2e displays the substrate microstructure below the interface under the as-deposited state. Fig. 2f is the microstructural feature of the substrate after 5hr aging. The substrate area shows equiaxed grains in both as-deposited and aged specimens. While the difference comes from the minor features in much higher amounts in the 5hr aging specimen, and in contrast, there is a limited amount in the as-deposited specimen. It was reported that the low-temperature aging of near-equiatomic TiNi alloy could create minor precipitates, especially Ni_4Ti_3 [10].

Fig. 2g-h are XRD results of the as-received TiNi substrate and the as-deposited Ti-rich Ti-Ni alloy. The major phase of the substrate area (Fig. 2g) matches the cubic TiNi B2 phase, while Fig. 2h displays the monoclinic TiNi B19′ phase within the DED Ti-Ni alloy section that corresponds to the Ti-rich martensitic phase. The DED process thus produced two different compositions and structures of Ti-Ni alloys that combined into a graded multi-functional SMA.

DSC curves of the graded Ti-Ni alloys at the interface, including both the as-deposited part and substrate, are demonstrated in Fig. 3. Fig. 3a-e represent DSC curves of as-deposited, 0.5hr, 1hr, 2hr, and 5hr aging. Two pairs of exothermic/endothermic peaks appear in Fig. 3a for the as-deposited situation, where M → A and A → M labels are marked for martensite-austenite and austenite–martensite transformation. The right peak pairs located at the higher temperature range reflect the Ti-rich DED section, while the low-temperature pairs come from the near-equiatomic substrate. Both the DED section and substrate section demonstrate single M → A and A → M peaks from the as-deposited specimen. Starting from Fig. 3b, the DED Ti-Ni alloy section maintained the single M → A and A → M transformation, while the substrate part obtained two peaks during cooling, which represents the formation of R-phase and the martensitic phase [11]. From Fig. 3b to Fig. 3e, all specimens show a single peak during cooling in the DED Ti-Ni section and double peaks in the TiNi substrate, which is the result of the 400 °C aging effects that created the formation of the Ni_4Ti_3 phase [12]. The as-deposited substrate part near the substrate underwent a high-temperature laser heating effect from DED. Therefore, the near interface substrate region under as-deposited state shows very few features from precipitate [13], as seen in Fig. 2e, which also corresponds to the lack of R-phase peak in Fig. 3a. Fig. 2f indicates much more precipitate features, which matches the observation of the large separation of R and martensite peaks seen in Fig. 3e.

Table 1 summarizes the austenite starting temperature (A_s) and the austenite finishing temperature (A_f) of two sections under the as-deposited state and all other aged states. In the DED section, the A_s and A_f values among different aging have very small effects from the aging time. The standard deviation of all five values of A_s and A_f are within 1 °C. This indicates the stability of the Ti-rich TiNi phase for low-temperature aging. In contrast, at the substrate region that is more sensitive to aging, the A_s and A_f both significantly increase with the increase in the aging time, especially the A_f ranging from 27.5 °C to 54.0 °C. The combination of various Ti-Ni SMAs can be realized by DED, where different sections can have different trends of austenite finishing temperature variation under the aging process. Therefore, a variety of TT combinations can be generated by DED followed by the aging process.

Fig. 4 shows the average hardness of locations L1 and L2 in all aging states. The average hardness at L1 within the DED section maintains stable, which indicates that the DED Ti-rich Ti-Ni alloy with ~ 51 at.% matrix has limited effects on phase changes from the aging effect at 400 °C, resulting in similar hardness values. For L2 in the near-equiatomic TiNi substrate, the as-deposited state obtains the lowest average hardness from the homogenous equiatomic TiNi phase. There is a significant increase in hardness from the as-deposited state to the 0.5hr aging state. Also, an increasing trend can be observed when the aging time increases. This might reflect the density of the precipitates such as Ni_4Ti_3 with precipitation hardening effect [14]. The high hardness after aging correlates well with the Ni_4Ti_3 effects and the R-phase formation in DSC curves.

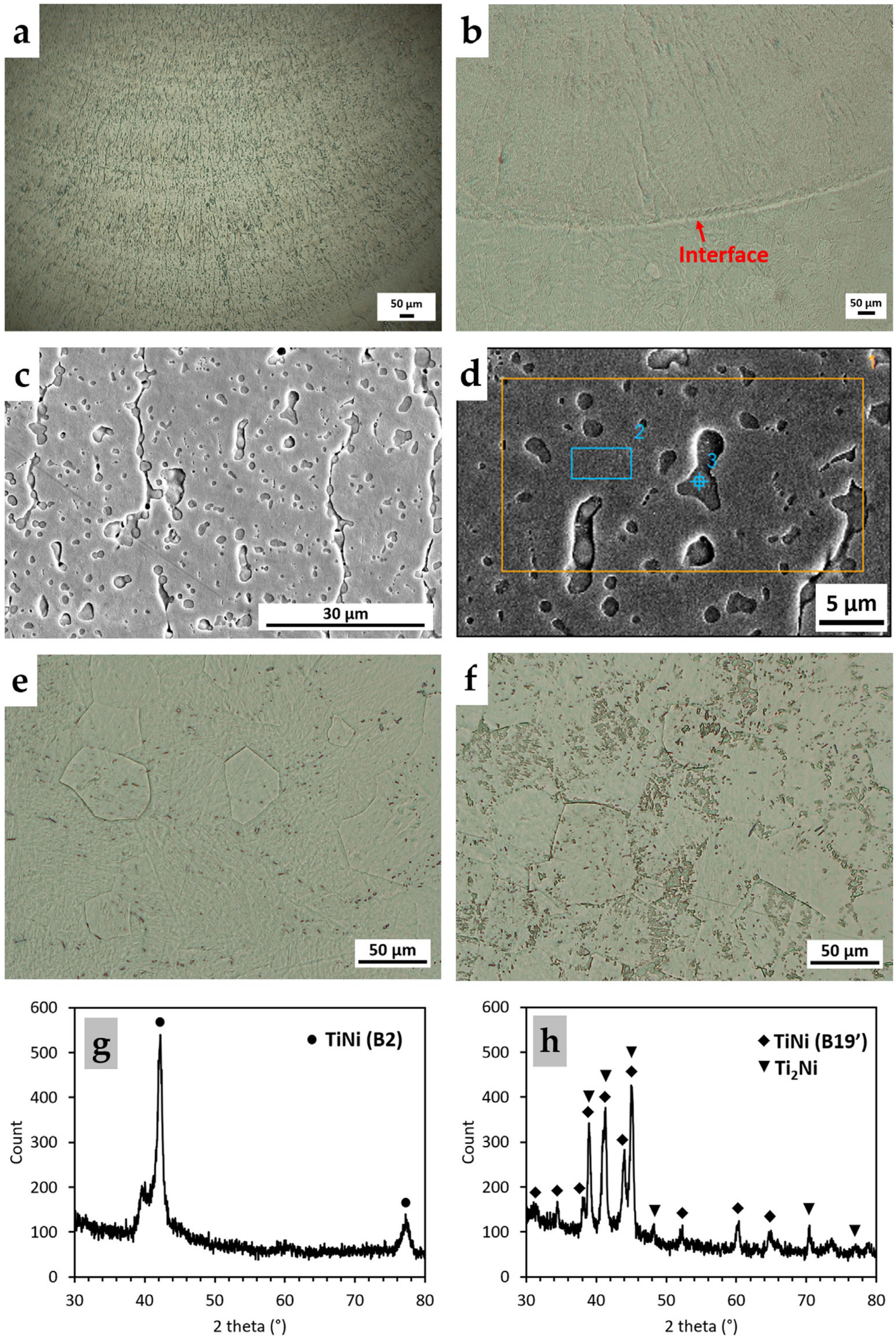

Fig. 2. (a) The OM image of DED Ti-Ni cross-section. (b) The interface between the DED Ti-Ni section and TiNi substrate. (c) SEM image of the DED Ti-Ni section with columnar structures. (d) The higher magnification of the DED Ti-Ni section for EDS analysis. (e) The OM image of the substrate below the interface with the as-deposited status. (f) The OM image of the substrate below the interface after 5hr aging. (g) XRD pattern of the substrate. (h) XRD pattern of the as-deposited Ti-Ni.

4. Conclusion

In this work, a graded Ti-Ni SMA was fabricated by laser-powder-DED with elemental powder, where the Ti-rich Ti-Ni alloy was deposited on the near-equiatomic TiNi substrate. The interface is clear with no defect. XRD revealed the structure differences between two sections. The DED section and substrate section show columnar and equiaxed grain structures, respectively. Precipitate features appear after aging, which corresponds to the variation in DSC curves and hardness. The as-deposited DED part got no

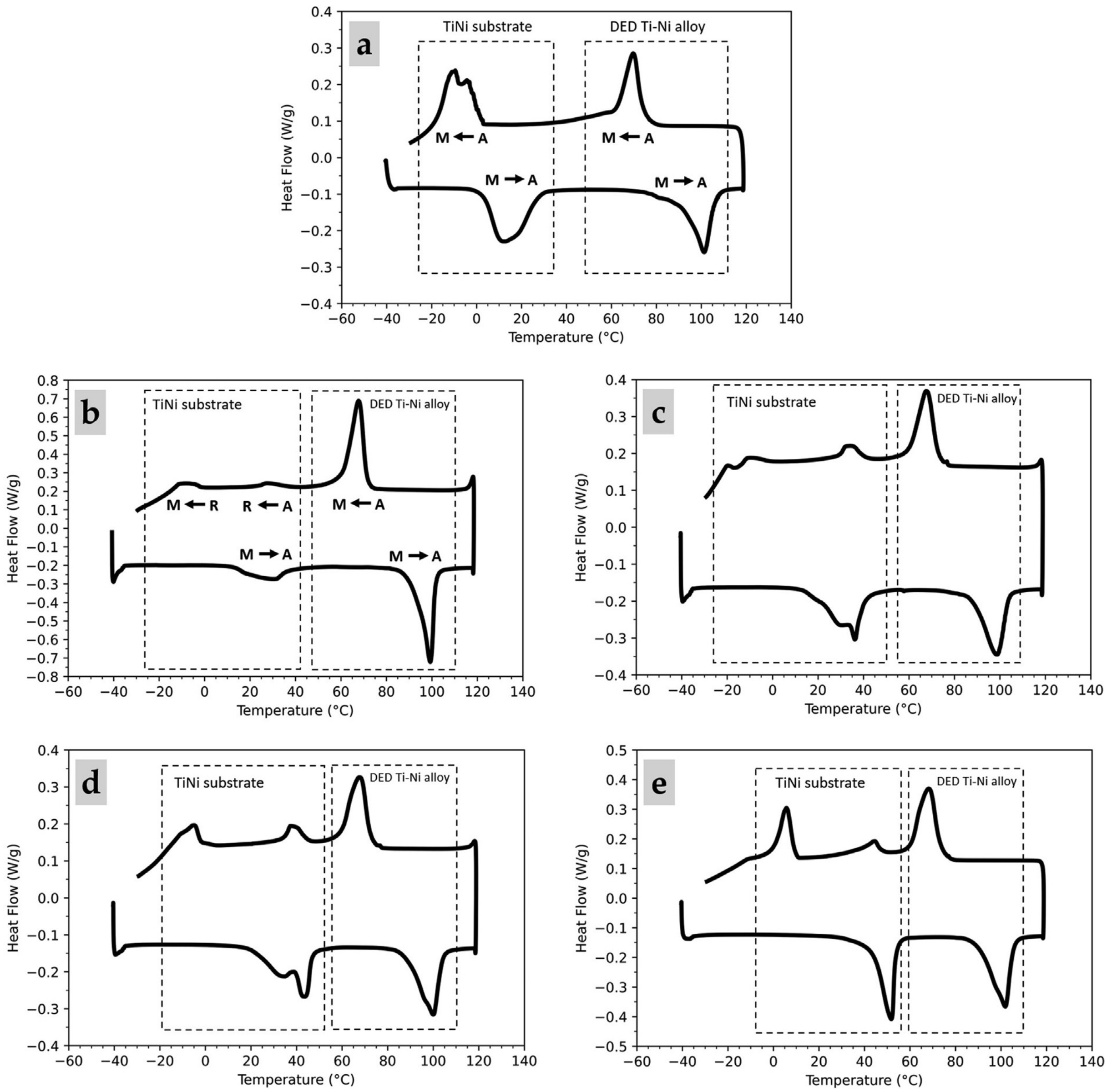

Fig. 3. DSC curves of two-section graded parts after aging: (a) 0hr (as-deposited). (b) 0.5hr. (c) 1hr. (d) 2hr. (e) 5hr.

Table 1
Characteristic temperature A_s and A_f of the two sections (°C).

	DED Ti-Ni section		TiNi substrate section	
	A_s	A_f	A_s	A_f
As-deposited	87.4	106.2	2.8	27.5
0.5hr	88.4	104.8	9.7	35.8
1hr	88.6	103.5	13.0	41.6
2hr	87.8	104.1	19.6	46.9
5hr	89.4	105.7	43.5	54.0

obvious changes in TTs and hardness after aging, while the near-equiatomic substrate significantly increased in A_f and hardness. DED shows a good method of joining multiple SMAs with different responses after aging, which can result in multiple shape memory effects and material properties. Future work can include aging time effects on DED graded SMA parts with more temperature levels.

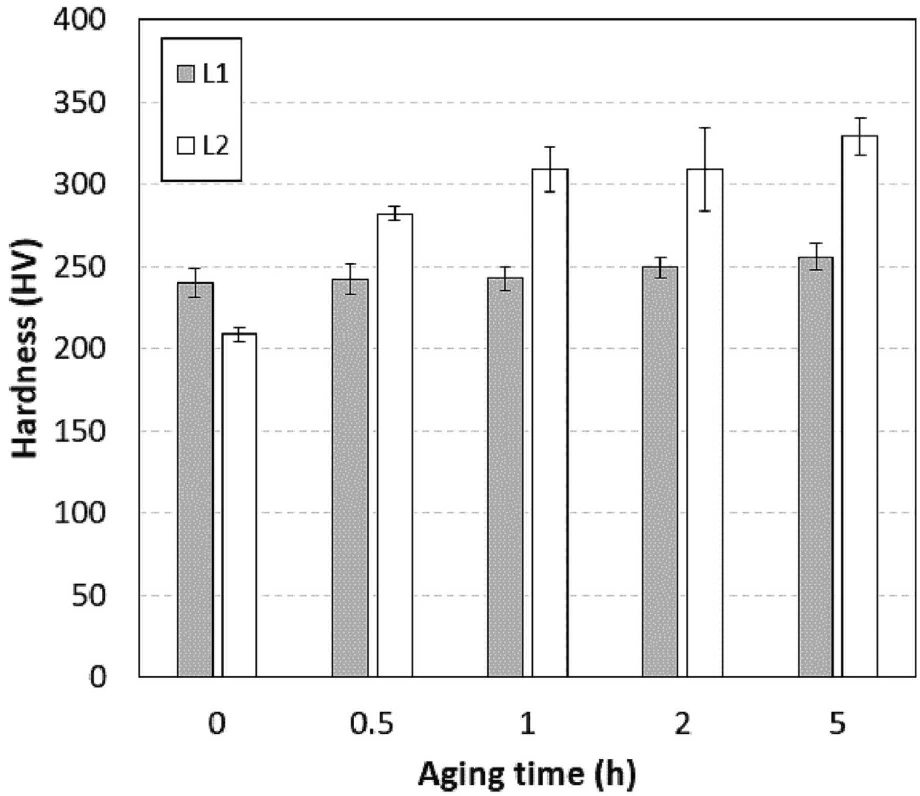

Fig. 4. The average hardness at L1 and L2 after 0hr, 0.5hr, 1hr, 2hr, and 5hr aging.

Declaration of Competing Interest

The authors declare that they have no known competing financial interests or personal relationships that could have appeared to influence the work reported in this paper.

Acknowledgement

This research was partially funded by the NSF Grants CMMI 1625736, NSF EEC 1937128, and Intelligent Systems Center and Material Research Center at Missouri S&T. Their financial support is greatly appreciated.

References

[1] Bennett J et al. Repairing automotive dies with directed energy deposition: industrial application and life cycle analysis. J Manuf Sci Eng 2019;141:2.
[2] Zhang X et al. Additive manufacturing of copper-tool steel dissimilar joining: Experimental characterization and thermal modeling. Mater Charact 2020;170:110692.
[3] Zheng M et al. The influence of columnar to equiaxed transition on deformation behavior of FeCoCrNiMn high entropy alloy fabricated by laser-based directed energy deposition. Addit Manuf 2021;37:101660.
[4] Fan W et al. Microstructures and mechanical properties of Invar/MnCu functionally graded material fabricated by directed energy deposition. Mater Sci Eng A 2022:144332.
[5] Bimber BA et al. Anisotropic microstructure and superelasticity of additive manufactured NiTi alloy bulk builds using laser directed energy deposition. Mater Sci Eng A 2016;674:125–34.
[6] Gao S et al. Molten pool characteristics of a nickel-titanium shape memory alloy for directed energy deposition. Opt Laser Technol 2021;142:107215.
[7] Chen Y et al. TiNi-Based Bi-Metallic Shape-Memory Alloy by Laser-Directed Energy Deposition. Materials 2022;15(11):3945.
[8] Halani PR et al. Phase transformation characteristics and mechanical characterization of nitinol synthesized by laser direct deposition. Mater Sci Eng A 2013;559:836–43.
[9] Yu L et al. Microstructures and mechanical properties of NiTi shape memory alloys fabricated by wire arc additive manufacturing. J Alloy Compd 2022;892:162193.
[10] Pandolfi GS et al. Precipitation kinetics of Ti3Ni4 and multistage martensitic transformation in an aged Ni–rich Ni–Ti shape memory alloy. J Mater Res Technol 2020;9(4):9162–73.
[11] Vashishtha H, Jain J. Influence of laser power on precipitate formation and multiple step transformation kinetics in NiTi shape memory alloy weld joints. J Alloy Compd 2022;893:162307.
[12] Adharapurapu RR. Phase transformations in nickel-rich nickel-titanium alloys: influence of strain-rate, temperature, thermomechanical treatment and nickel composition on the shape memory and superelastic characteristics. San Diego: University of California; 2007.
[13] Zheng Y et al. Effect of ageing treatment on the transformation behaviour of Ti–50.9 at.% Ni alloy. Acta Materialia 2008;56(4):736–45.
[14] Nurveren K, Akdoğan A, Huang WM. Evolution of transformation characteristics with heating/cooling rate in NiTi shape memory alloys. J Mater Process Technol 2008;196(1-3):129–34.